Science Advances
AAAS

advances.sciencemag.org/cgi/content/full/6/3/eaax9051/DC1

Supplementary Materials for

Atmospheric fungal nanoparticle bursts

Michael J. Lawler*, Danielle C. Draper, James N. Smith

*Corresponding author. Email: mlawler@uci.edu

Published 15 January 2020, *Sci. Adv.* **6**, eaax9051 (2020)
DOI: 10.1126/sciadv.aax9051

This PDF file includes:

Fig. S1. Partial time series of selected detected ions in positive mode from ambient nanoparticles sampled over agricultural land in northern Oklahoma.
Fig. S2. Characteristic positive ion mass spectra for nanoparticles sampled during the study.
Fig. S3. Time series of chitin monomer detected in positive (red trace) and negative (blue trace) ion modes from ambient nanoparticles.
Fig. S4. Linear correlation plot comparing rainfall and TDCIMS chitin signal.
Fig. S5. TDCIMS desorption thermograms for individual high-resolution fitted positive ions for the event collection period on 15 September and the positive non-event collection preceding it (Fig. 1).
Fig. S6. Aerosol size distributions and IN concentrations measured in a previous study at the same site during a high IN event.
Fig. S7. Integrated ion counts for the chitin monomer ($C_8H_{14}NO_5^+$) plotted against integrated ion counts for $C_6H_{15}O_6^+$ (mannitol isomer) detected in ~20- to 50-nm particles by TDCIMS in positive ion mode.
References (*57*, *58*)

Supplementary Materials to Atmospheric Fungal Nanoparticle Bursts (Lawler et al. 2019):

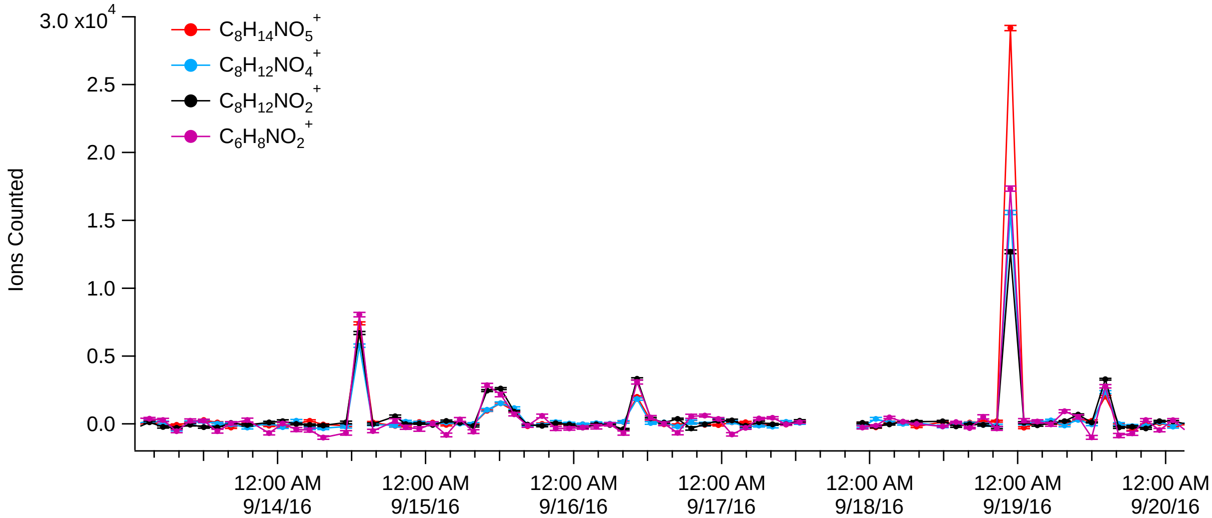

Fig. S1. Partial time series of selected detected ions in positive mode from ambient nanoparticles sampled over agricultural land in northern Oklahoma. These four ions are characteristic chitin fragments generated by pyrolysis of the sampled aerosol and detected by time-of-flight chemical ionization mass spectrometry. One standard error bars are plotted.

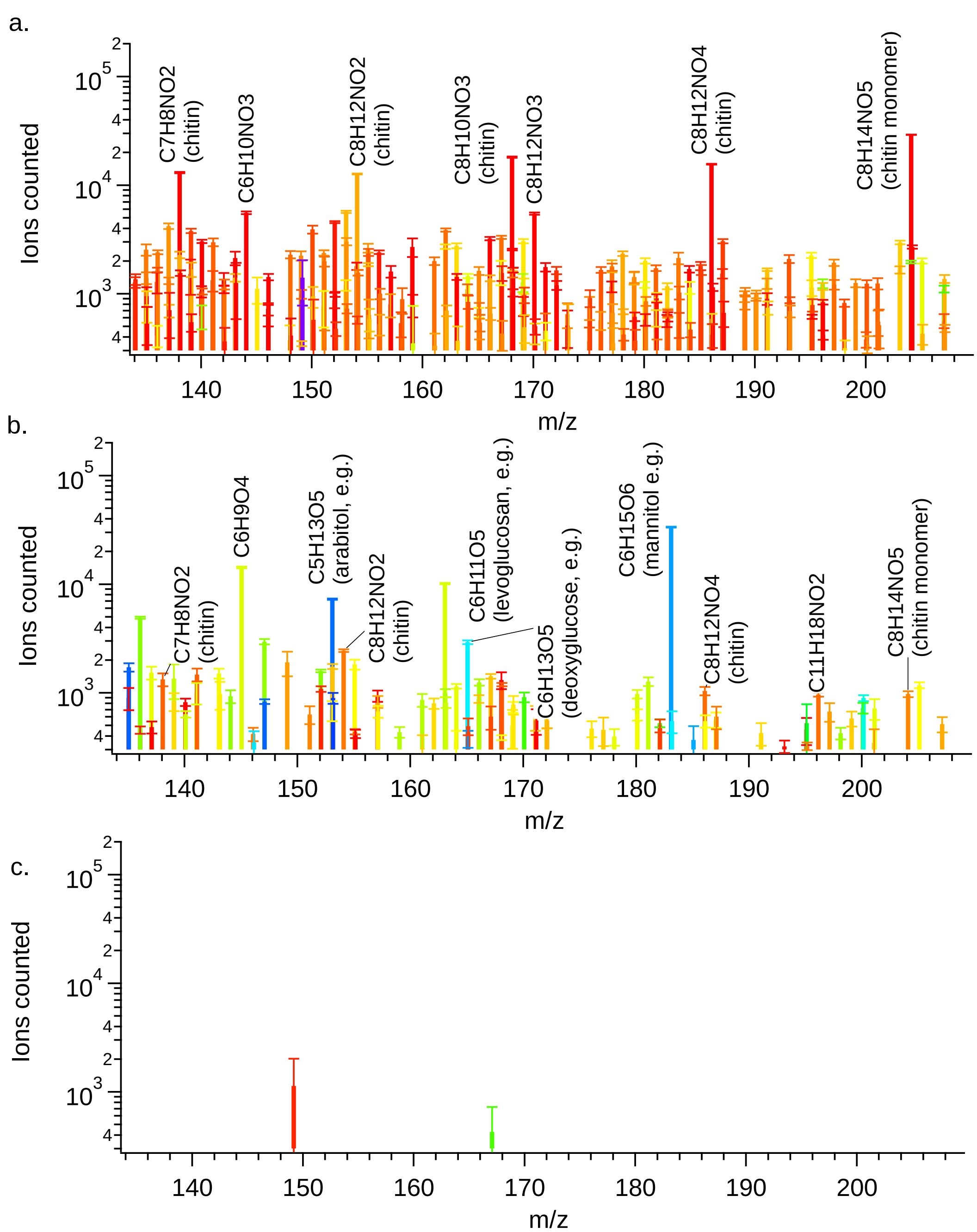

Fig. S2. Characteristic positive ion mass spectra for nanoparticles sampled during the study. a.) Mass spectrum of an event period collection (Sept 18, 2016) with detected peaks dominated by chitin. b.) Mass spectrum of the event period presented in the main manuscript (fig. 1), from Sept 15, 2016. Detected peaks include chitin but signal is dominated by free sugar alcohols. c.) Mass spectrum of the non-event period preceding the Sept 15th event. Colors indicate the timing of the peaks during the filament temperature ramp. Orange and red colors indicate the products of the pyrolytic breakdown of larger molecules, including polymers like chitin. Cooler colors (blue) indicate molecules which likely desorbed intact. Molecular formulae consistent with chitin pyrolysis products and desorbed sugars are indicated.

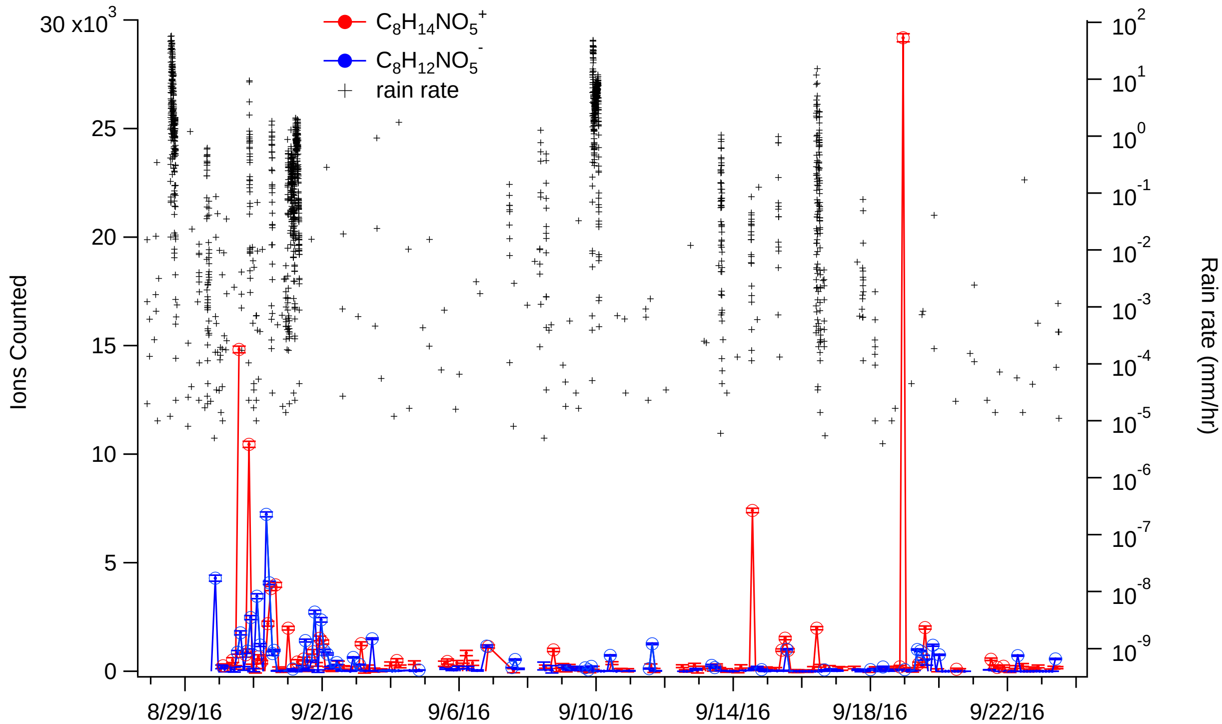

Fig. S3. Time series of chitin monomer detected in positive (red trace) and negative (blue trace) ion modes from ambient nanoparticles. Open circles are detectable chitin signal. Black crosses are one-minute-averaged rain rate. The most active fungal nanoparticle period occurred during and following the rainiest period of the campaign, at the end of August.

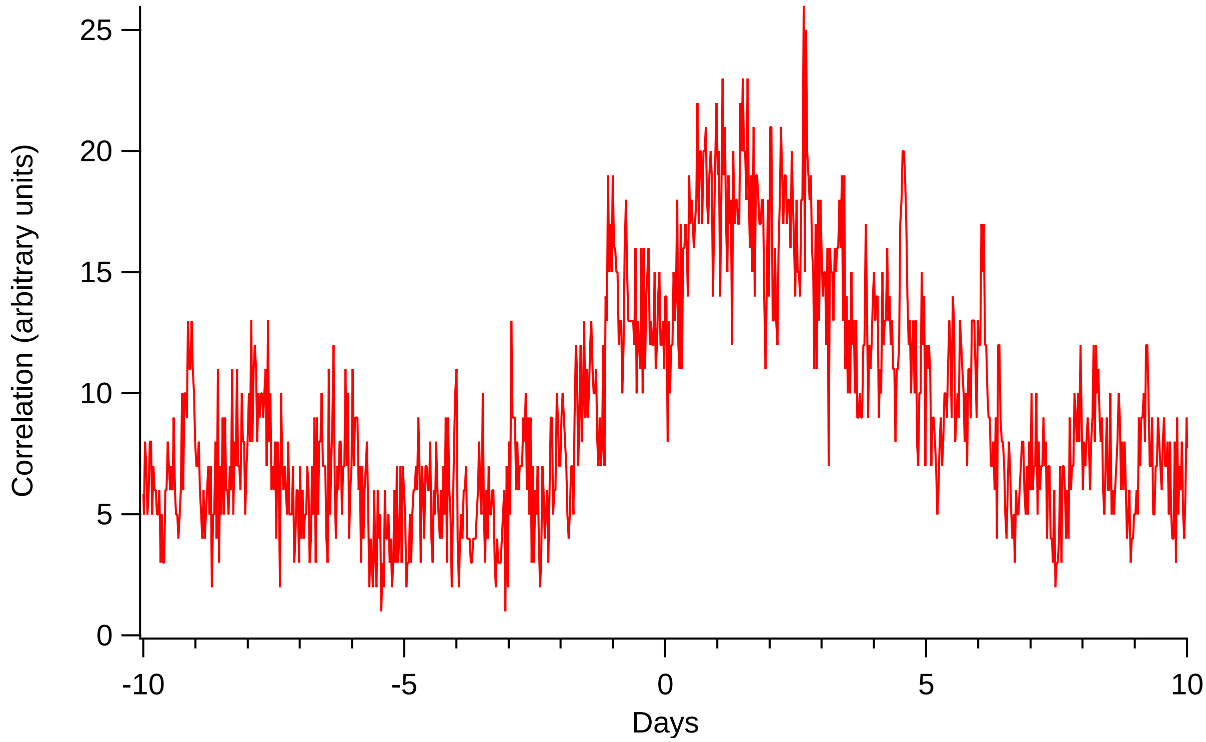

Fig. S4. Linear correlation plot comparing rainfall and TDCIMS chitin signal. Rainfall was averaged on the same time basis as the TDCIMS collection periods. If a time period had detectable rain, it was assigned a value of 1, and otherwise zero. If a time period had detectable chitin signal, in either TDCIMS ion mode, it was assigned a value of 1, otherwise zero. Correlations are highest during and following rain events.

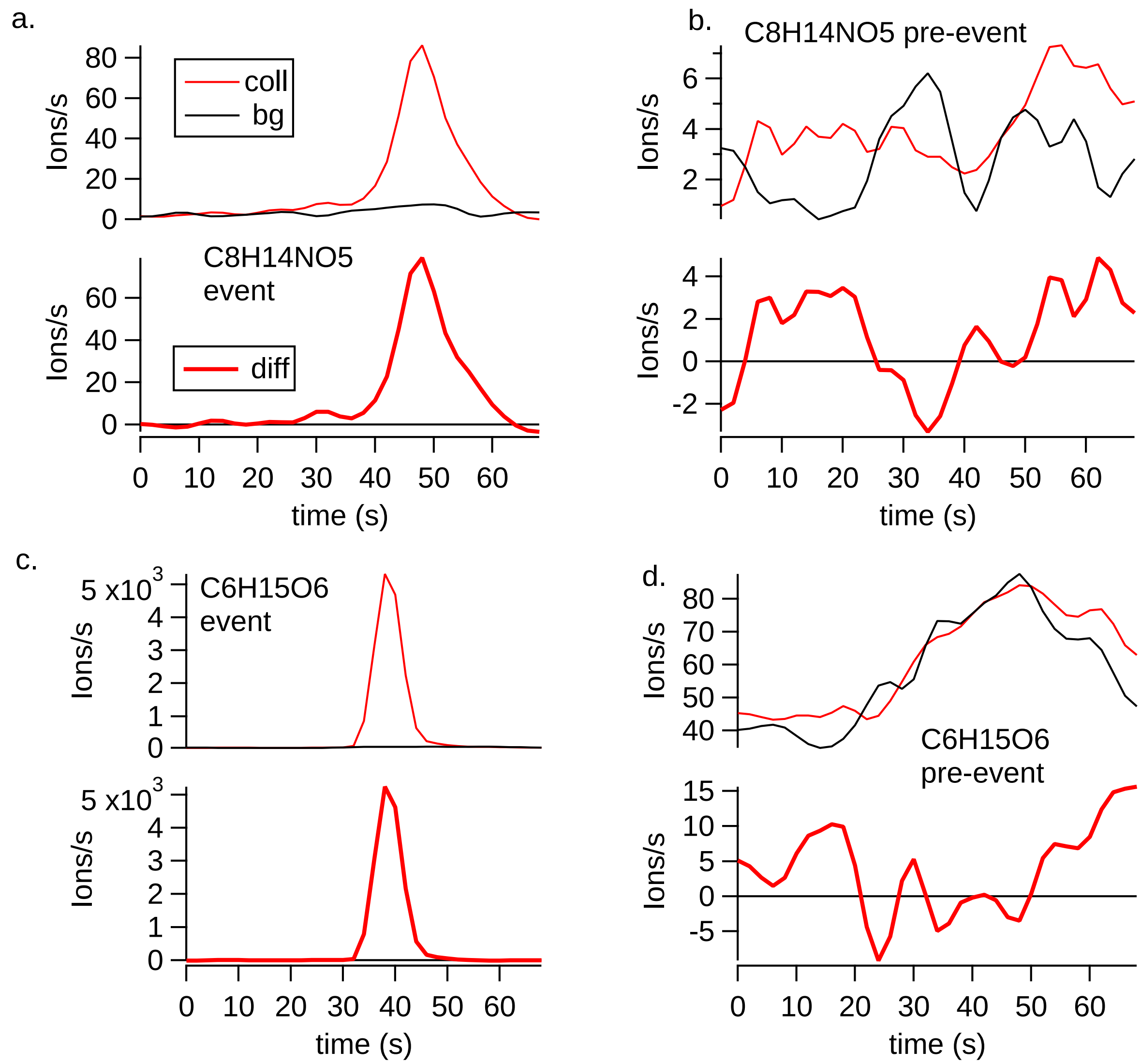

Fig. S5. TDCIMS desorption thermograms for individual high-resolution fitted positive ions for the event collection period on 15 September and the positive non-event collection preceding it (Fig. 1). Event period a.) chitin monomer detected as $C_8H_{14}NO_5^+$ and c.) mannitol detected as $C_6H_{15}O_6^+$ and non-event period b.) chitin and d.) mannitol. These two compounds were clearly detectable during the event but not in the preceding aerosol collection. Mannitol desorbs earlier in the temperature ramp, and chitin pyrolyzes at a higher temperature.

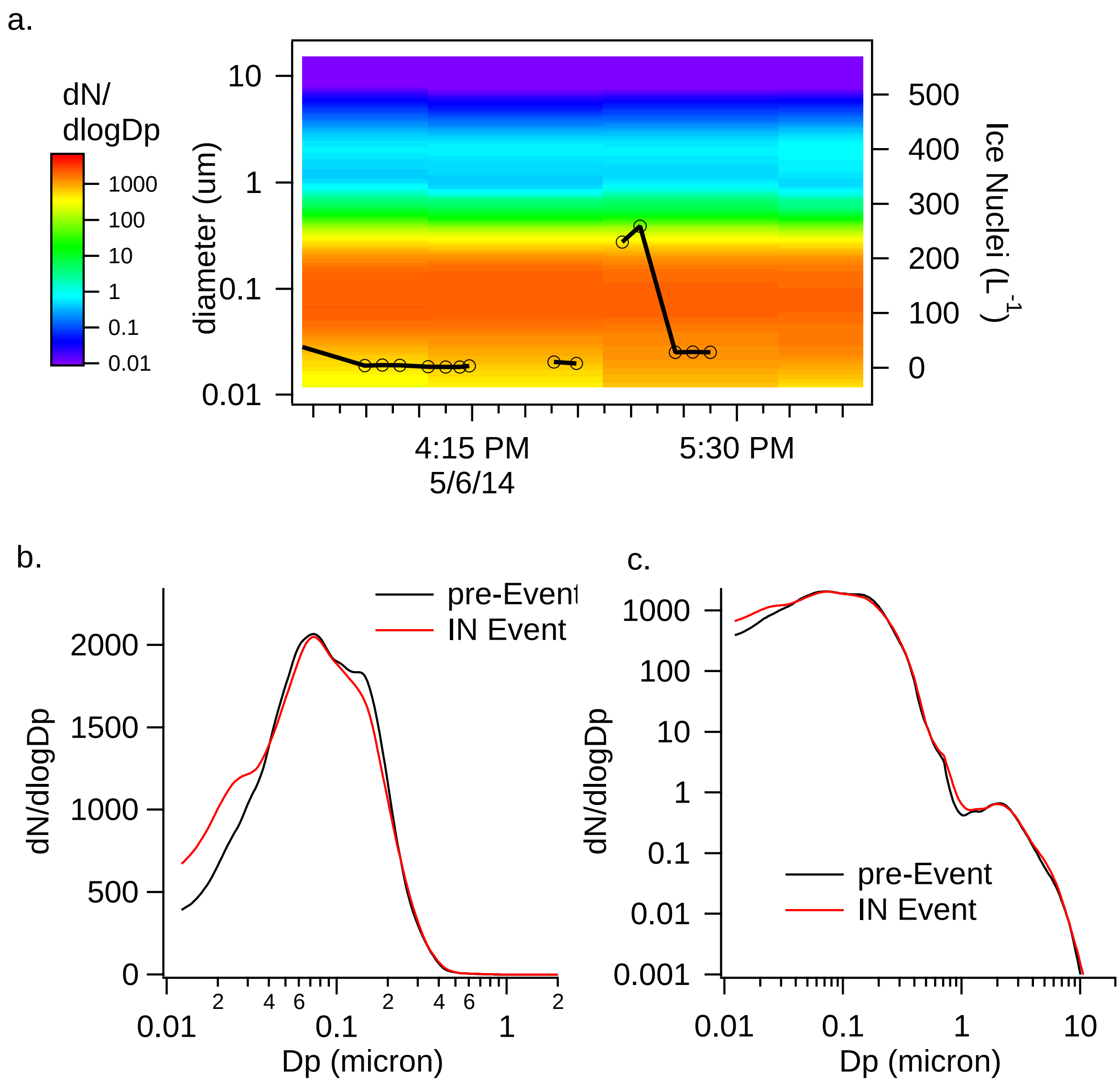

Fig. S6. Aerosol size distributions and IN concentrations measured in a previous study at the same site during a high IN event. a.) IN concentration as measured by Continuous Flow Diffusion Chamber at the ARM SGP site in May 2014 (black circles and traces) (*53*), and ambient aerosol particle size distributions, as measured by a combination of aerosol particle sizer and scanning mobility particle sizer (*54*). b.) Aerosol size distributions for the period encompassing the IN event and the previous measurement. c.) Same size distribution as (b.), presented in log space to show dynamics at large sizes and small concentrations. The increase in particle number during the IN event is 0.26 cm^{-3} for aerosol of 0.5-1.5 µm diameter, and is 102 cm^{-3} for aerosol of 0.01- 0.05 µm diameter. The average increase in IN between these two aerosol size periods is 0.11 cm^{-3}, based on an estimated aerosol concentration factor for 1 micron particles, using an aerosol concentrator which optimizes for that size at the cost of smaller sizes.

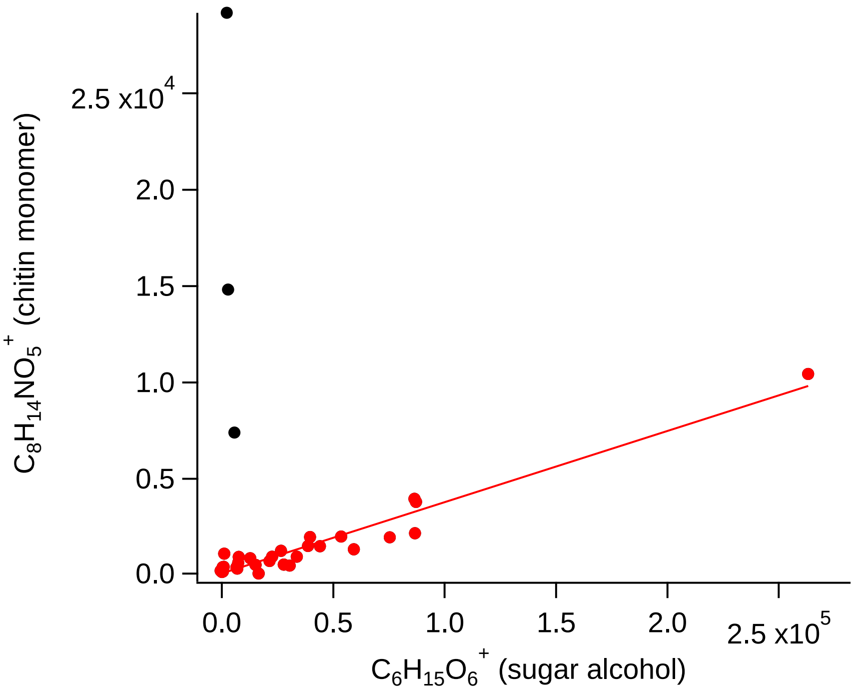

Fig. S7. Integrated ion counts for the chitin monomer ($C_8H_{14}NO_5^+$) plotted against integrated ion counts for $C_6H_{15}O_6^+$ (mannitol isomer) detected in ~20- to 50-nm particles by TDCIMS in positive ion mode. Only points with detectable chitin signal are shown. Three points (black circles) showed significantly higher chitin:mannitol ratios than the others, suggesting a source or process distinct from the others. If these points are removed, the remaining points (38 of 41 samples, red circles) showed a strong linear relationship (r^2= 0.93), suggesting that these events were from similar fungal materials.